Mon. Not. R. Astron. Soc. **000**, 1–11 (2015) Printed 23 May 2016 (MN LATEX style file v2.2)

XMM-Newton discovery of mHz quasi-periodic oscillations in the high mass X-ray binary IGR J19140+0951

L. Sidoli,[1⋆] P. Esposito,[1,2] S. E. Motta,[3] G. L. Israel,[4] and G. A. Rodríguez Castillo,[4]
[1]*INAF, Istituto di Astrofisica Spaziale e Fisica Cosmica, Via E. Bassini 15, I-20133 Milano, Italy*
[2]*Anton Pannekoek Institute for Astronomy, University of Amsterdam, Postbus 94249, NL-1090-GE Amsterdam, The Netherlands*
[3]*Department of Physics, Astrophysics, Denys Wilkinson Building, University of Oxford, Keble Road, Oxford OX1 3RH, UK*
[4]*INAF, Osservatorio Astronomico di Roma, Via Frascati 33, I-00040 Monteporzio Catone, Italy*

arXiv:1605.06356v1 [astro-ph.HE] 20 May 2016

Accepted Received

ABSTRACT

We report on the discovery of mHz quasi-periodic oscillations (QPOs) from the high mass X-ray binary (HMXB) IGR J19140+0951, during a 40 ks *XMM-Newton* observation performed in 2015, which caught the source in its faintest state ever observed. At the start of the observation, IGR J19140+0951 was at a low flux of 2×10^{-12} erg cm^{-2} s^{-1} (2-10 keV; L_X=3×10^{33} erg s^{-1} at 3.6 kpc), then its emission rised reaching a flux $\sim$10 times higher, in a flare-like activity. The investigation of the power spectrum reveals the presence of QPOs, detected only in the second part of the observation, with a strong peak at a frequency of 1.46$\pm$0.07 mHz, together with higher harmonics. The X–ray spectrum is highly absorbed (N_H=10^{23} cm^{-2}), well fitted by a power-law with a photon index in the range 1.2-1.8. The re-analysis of a *Chandra* archival observation shows a modulation at $\sim$0.17$\pm$0.05 mHz, very likely the neutron star spin period (although a QPO cannot be excluded). We discuss the origin of the 1.46 mHz QPO in the framework of both disc-fed and wind-fed HMXBs, favouring the quasi-spherical accretion scenario. The low flux observed by XMM-Newton leads to about three orders of magnitude the source dynamic range, overlapping with the one observed from Supergiant Fast X–ray Transients (SFXTs). However, since its duty cycle is not as low as in SFXTs, IGR J19140+0951 is an intermediate system between persistent supergiant HMXBs and SFXTs, suggesting a smooth transition between these two sub-classes.

Key words: accretion - stars: neutron - X–rays: binaries - X–rays: individual (IGR J19140+0951)

1 INTRODUCTION

IGR J19140+0951 (formerly known as IGR J19140+098) was discovered in 2003 March during an *INTEGRAL* observation targeted on the microquasar GRS 1915+105 (Hannikainen et al. 2003, 2004). A follow-up observation with *RossiXTE* PCA detected the source at 10^{-10} erg cm^{-2} s^{-1} (2–10 keV) and 2×10^{-10} erg cm^{-2} s^{-1} (10–60 keV). The source was variable on timescales longer than 100 s, with a power-law spectrum (N_H=6×10^{22} cm^{-2}, photon index, Γ, of 1.6) and an iron line complex (equivalent width EW=550 eV; Swank & Markwardt 2003). The flux dynamic range of 150 in the energy band 1-20 keV (Rodriguez et al. 2006), the iron line and the absorbing column density properties were interpreted as indicative of an HMXB nature (Rodriguez et al. 2005; Hannikainen et al. 2004; Prat et al. 2008). This suggestion was strengthened by the discovery of a periodicity of 13.558(4) days (epoch of maximum flux on MJD 51593.4$\pm$0.32) in the *RossiXTE* ASM light curve, likely the orbital period of the system (Corbet et al. 2004). A refined period of 13.552(3) days was later determined by Wen et al. (2006), again analysing *RossiXTE* ASM data.

The confirmation that IGR J19140+0951 is indeed an HMXB came from the identification of the optical counterpart, the star 2MASS 19140422+0952577, which was possible thanks to the *Chandra* sub-arcsec X–ray position (in't Zand et al. 2006). Several authors investigated its optical/infrared properties (in't Zand et al. 2006, Nespoli et al. 2007, Hannikainen et al. 2007, Chaty et al. 2008, Rahoui et al. 2008, Nespoli et al. 2008, Torrejón et al. 2010), all confirming an early-type supergiant companion. The most recent optical photometry performed by Torrejón et al. (2010) indicates a B0.5 Ia star located at a distance of $\sim$3.6 kpc.

The possible identification with the X–ray source EXO 1912+097 (Lu et al. 1996, Lu et al. 1997), suggested by several authors (Hannikainen et al. 2004, Hannikainen et al. 2007, in't Zand et al. 2004, 2006) appears rather uncertain (see

⋆ E-mail: sidoli@iasf-milano.inaf.it

Section 4.1 for a discussion of the available literature). However, $RossiXTE$ ASM (Corbet et al. 2004) and $BeppoSAX$ WFC (in't Zand et al. 2004) detected it at earlier times, before the $INTEGRAL$ discovery.

Since the absorbing column density is an order of magnitude higher than the interstellar one (Nespoli et al. 2008; Prat et al. 2008), IGR J19140+0951 was suggested to belong to the so-called "highly obscured HMXBs" unveiled by $INTEGRAL$ satellite (Kuulkers 2005).

In this *paper*, we report on the discovery of mHz quasi-periodic oscillations (QPOs) in an *XMM-Newton* observation performed in 2015 October, together with a re-analysis of $Chandra$ archival data.

2 OBSERVATIONS AND DATA REDUCTION

2.1 *Chandra*

A *Chandra* observation of IGR J19140+0951 was carried out on 2004 May 11 (obs. ID 4590) for a total exposure time of 20.1 ks (in't Zand et al. 2006). The source was positioned in the back-illuminated ACIS-S3 CCD and the instrument was operated in full-imaging timed-exposure mode (with no gratings), with a frame time of 3.24 s. We generated new level 2 event files the *Chandra* Interactive Analysis of Observations (CIAO) software version 4.7 and following standard procedures. Since our results for the spectral analysis are essentially consistent with those of in't Zand et al. (2006), to which we refer the reader, in this paper we give only some details on the timing analysis that led to the discovery of the modulation of IGR J19140+0951 (Section 3.1).

2.2 *XMM-Newton*

The *XMM-Newton* $Observatory$ carries three 1500 cm^2 X–ray telescopes, each with an European Photon Imaging Camera (EPIC) detector at the focus. Two of the EPIC detectors use MOS CCDs (Turner et al. 2001) and one uses pn CCDs (Strüder et al. 2001). Reflection Grating Spectrometer (RGS; 0.4-2.1 keV) arrays (den Herder et al. 2001) are located in the telescopes with MOS cameras at their primary focus.

The source position was observed by *XMM-Newton* on 2015, October 26-27, for a net exposure of 40.2 ks (Obs. ID 0761690301). The EPIC pn camera was operated in full frame mode, while both the MOS cameras were in small window mode. The data were reprocessed using version 14 of the Science Analysis Software (SAS) with standard procedures. Given the high absorption in the source direction which severely affected the observed emission up to 2 keV, the RGS data led to insufficient counts to afford a meaningful spectroscopy, so we will not discuss them further.

The EPIC field of view (FOV) was contaminated by the stray light coming from a bright source outside the FOV (Fig. 1), very likely the microquasar GRS 1915+105.

For the spectral analysis, we used EPIC data. We extracted source counts from circular regions with radii of 25″ radius (EPIC pn and MOS2) and 30″ radius (MOS1), using PATTERN from 0 to 4 (mono- and bi- pixel events) in the pn, and from 0 to 12 (up to 4-pixel events) in both MOS cameras. Background counts were obtained from similar circular regions, offset from the source position. Since the pn operated in full frame mode, it was possible to optimize the choice for the background region nearby the source, to subtract better the stray light contamination (see Fig. 1).

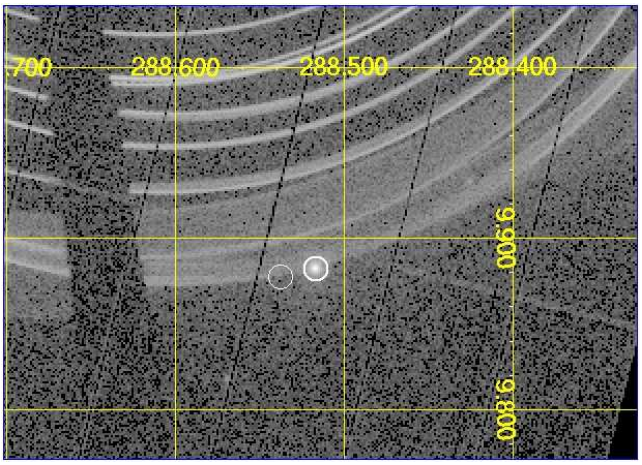

Figure 1. Close-up view of the central part of the EPIC pn image (2-12 keV). Sky coordinates are R.A. and Dec (J2000). Two white circles mark the extraction regions for the background (thin circle) and the source counts (thick circle). Stray light contamination from a bright source outside the FOV is evident.

Background regions from different CCDs, farther away from the source, were selected in both MOS cameras, which were operated in small window mode. However, the choice of the background spectra seemed not to affect significantly the spectral results: we obtained similar spectral parameters fitting only pn spectrum compared to analysis of the joint pn and MOS spectra together.

The background level was stable along the observation, so no further filtering was applied. Appropriate response matrices were generated using the SAS tasks ARFGEN and RMFGEN. All spectral uncertainties are given at 90% confidence level for one interesting parameter. Spectra were grouped so to have a minimum of 25 counts per bin. We fitted the three EPIC spectra simultaneously, adopting normalization factors to account for uncertainties in instrumental responses. Fluxes are quoted adopting the pn camera response matrix. In the spectral fitting we adopted the interstellar abundances of Wilms et al. (2000) and photoelectric absorption cross-sections of Balucinska-Church & McCammon (1992), using the absorption model TBABS in XSPEC.

3 ANALYSIS AND RESULTS

3.1 Timing analysis of *Chandra* data

In the 2004 *Chandra* observation of IGR J19140+0951, in't Zand et al. (2006) noticed a possible modulation with a period of about 6.5 ks. Indeed, a signal at a similar period (∼5.9 ks) was discovered by the detection algorithm of the *Chandra ACIS Timing Survey* (CATS) project[1] during an authomatic search of the same data set (Israel et al., submitted; see also Esposito et al. 2013, 2015).

Fig. 2 shows the Fourier periodogram that led to the discovery of the signal in IGR J19140+0951, normalized according to Leahy et al. (1983). The number of searched frequencies is 8192. A peak at frequency $\nu \simeq 0.168$ mHz ($P = 1/\nu \simeq 5\,950$ s) stands

[1] The CATS project is a Fourier-transform-based systematic and automatic search for new pulsating sources in the *Chandra* ACIS public archive. So far more than half a million light curves were analyzed and the effort yielded dozens of previously unknown X-ray pulsators.

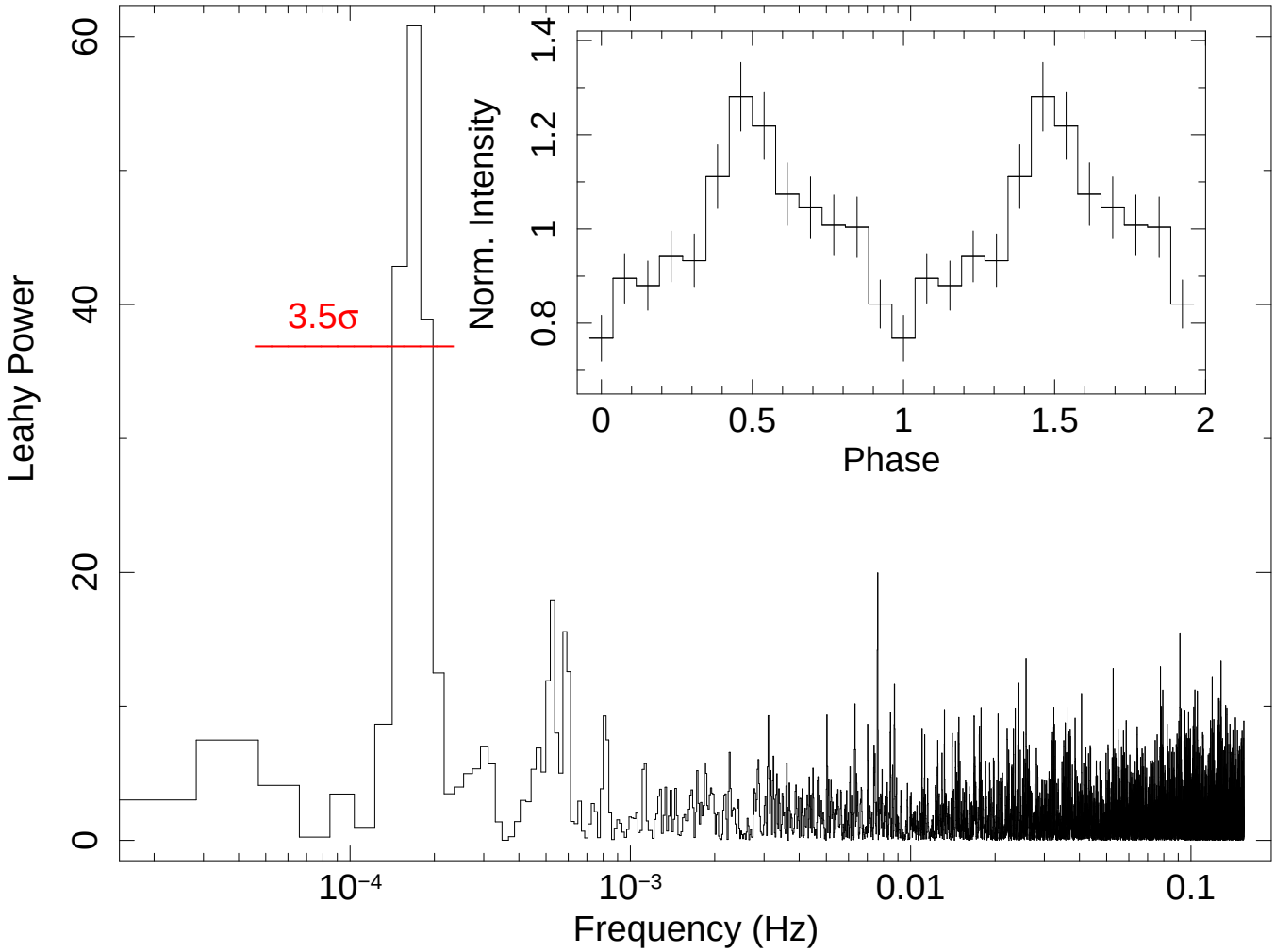

Figure 2. Power spectrum of IGR J19140+0951 computed from the *Chandra*/ACIS data of 2004 May 11 (0.5–10 keV). The red horizontal line indicates the 3.5σ significance level, which is essentially constant at all frequencies. The inset shows the light curve folded at the period we measured ($P = 5\,937$ s).

above the 3.5σ significance level, which was estimated taking into account the number of frequencies searched and the noise components of the spectrum following Israel & Stella (1996). Given the small number of modulation cycles sampled by the *Chandra* observation (roughly 3.5), to measure the period we simply fitted a sinusoid curve to the *Chandra* light curve. This returned the value $P = 5\,937 \pm 219$ s (90% confidence level). The inset of Fig. 2 shows the light curve folded at this period. A pulsed fraction (defined as the semi-amplitude of the sinusoid divided by the average count rate) of 20±3% was inferred from the fit.

The quality factor of the signal (defined as $Q = \nu/\Delta\nu$, the ratio of the frequency ν of the peak to its full width at half-maximum $\Delta\nu$) $Q \simeq 3$ is comparable to the typical values of QPOs. However, we notice that the low Fourier resolution of our data (see Fig. 2) would not allow us to distinguish the case of a QPO from that of a strictly coherent pulsation around 0.1 mHz. Furthermore, see the discussion in Sect. 4.4 supporting the interpretation of this signal as the NS spin period. The source flux during the *Chandra* observation was around 10^{-10} erg cm^{-2} s^{-1} (in't Zand et al. 2006), translating into an X-ray luminosity of $\sim 10^{35}$ erg s^{-1} at 3.6 kpc.

3.2 Timing analysis of *XMM-Newton* data

The IGR J19140+0951 EPIC pn background-subtracted light curve in two energy ranges is shown in Fig. 3. It starts with a low, although quite variable, emission. Then a flare-like behaviour is present in the second half of the observation. Folding the whole light curve at the periodicity found in the $Chandra$ observation, a modulation is evident in the data. However, it does not provide conclusive proof that the modulation found in *Chandra* data is present also in the *XMM-Newton* data, since folding EPIC light curve at diffent values of the putative period, results in apparent modulation as well. Moreover, *XMM-Newton* data are not constraining, as the upper limit on the pulsed fraction is >100%.

We performed the timing analysis of IGR J19140+0951 computing the power density spectra (PDS) from the EPIC pn data using custom software under IDL in the full EPIC pn energy band (0.1-10 keV). We produced one single PDS for the entire dataset (Fig. 4), between 0.03 mHz (our frequency resolution) and the maximum possible Nyquist frequency (∼6.8 Hz, set by the time resolution of our observation, ∼0.073 s), normalized according to Leahy et al. (1983) and converted to square fractional rms (Belloni & Hasinger 1990). We did not subtract the contribution due to Poissonian noise, but we fitted it afterwards.

The total fractional variability of the PDS is surprisingly high,

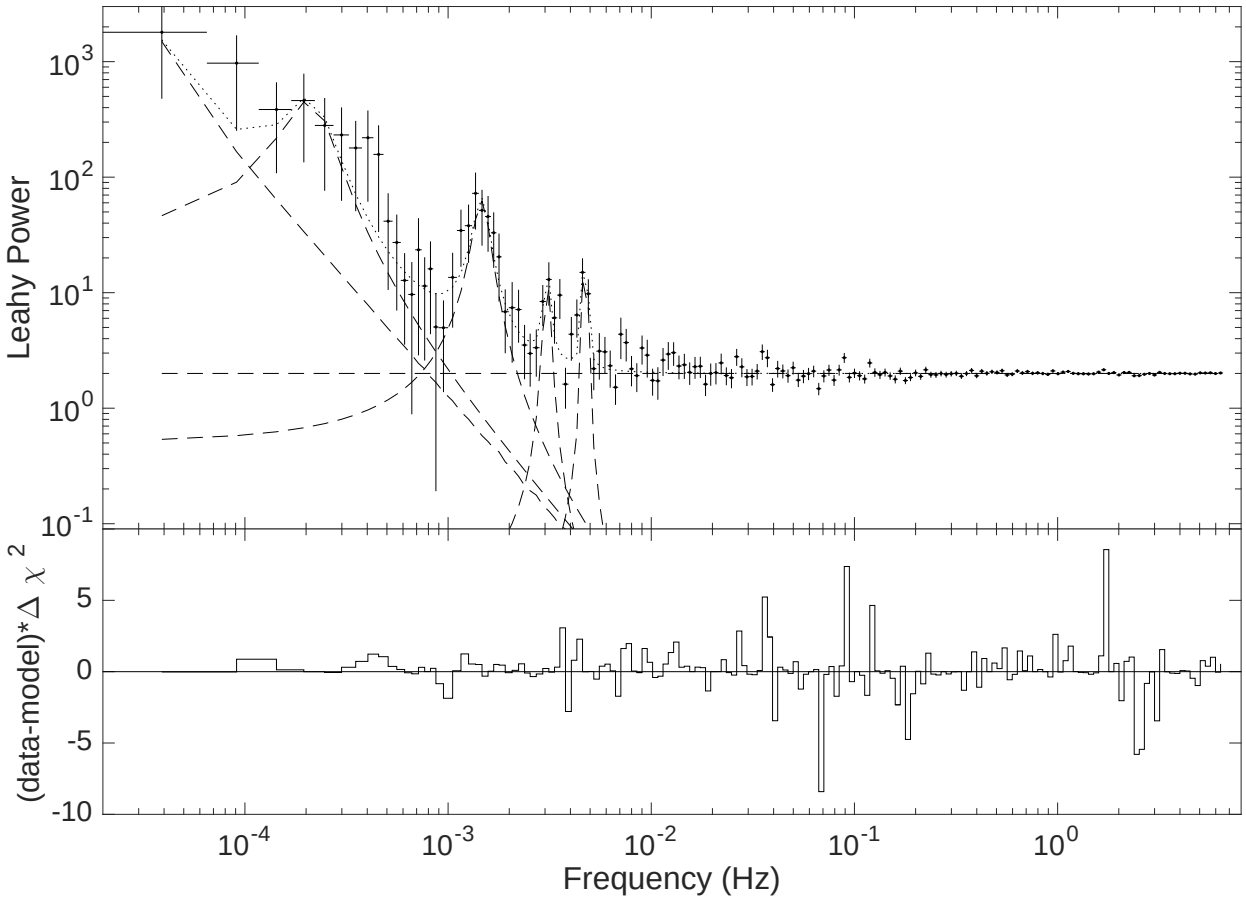

Figure 4. Power spectrum of IGR J19140+0951 computed from the whole *XMM-Newton* EPIC pn data of 2015 (0.1–10 keV).

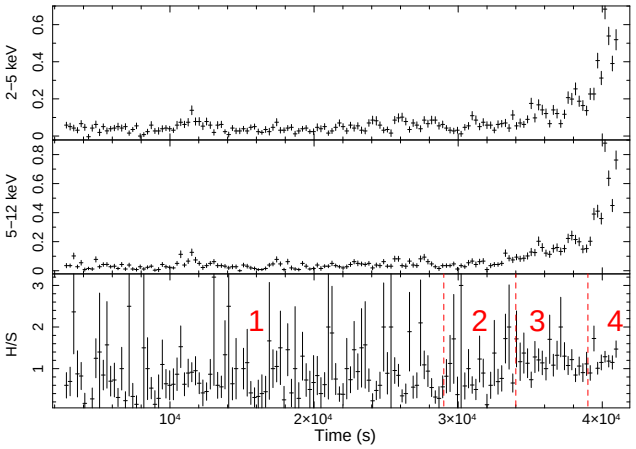

Figure 3. IGR J19140+0951 EPIC pn background subtracted X–ray light curves (below and above 5 keV; bin time 256 s), together with their hardness ratio. Numbers in the lower panel mark the four time intervals chosen for the temporal selected spectroscopy.

with almost 93 % of the emission variable. The PDS shows a broad-band, possibly flat-top noise component and a clear fairly narrow feature at ∼1.5 mHz, with two other narrow features, apparently harmonically related to the first one. We carried out the PDS fitting with the XSPEC fitting package by using a one-to-one energy-frequency conversion and a unit response. Following Belloni et al. (2002), we fitted the noise components with a suitable number of broad Lorentzians (in this case one zero-centred broad Lorentzian and a narrower one at slightly higher frequencies), while we fitted the QPO peaks with narrow Lorentzians. Even though the three QPO peaks seem to be harmonically related, we did not link the peak frequencies in the fit. A constant component was added to the model to take into account the contribution of the Poissonian noise. Our fit shows that the strongest peak is highly significant (4σ) and is centered at 1.46 ± 0.07 mHz, with a FWHM of 0.25 mHz ±0.07 Hz and amplitudes $42(\pm5)$% rms. The second and third harmonics are detected with a 2.3 and 3.4 σ significance, respectively, at frequencies consistent with being harmonics of the strongest peak. The QPO and its harmonics are only detected in the second part of our observation, in correspondence of the large flare starting at about 30 ks from the observation start, while only broad band noise and Poisson noise are visible in the first half of the observation. Since the QPO is detected at very low frequency, the total exposure of our observation limits our analysis and prevents us from a further investigation of the transient nature of this feature. We also notice

that the QPO shows a dependence on energy, being clearly present only above 3 keV.

Since our observation is affected by stray lights caused by the presence of a close-by bright source out of the FOV (probably the bright black hole (BH) binary GRS 1915+105), we performed some additional timing analysis on the background emission as well, in order to exclude possible contamination from GRS 1915+105 or other sources in the field. Following the steps outlined above, we computed PDS from the background emission, both close to the source and on a CCD region that is highly contaminated by the stray lights emission. In both cases, we did not detect any significant variability from the background, neither as a broadband noise nor in the form of a narrow feature. Therefore, we can reasonably exclude that the QPO is of instrumental origin or due to contamination from another, variable, source.

3.3 *XMM-Newton* spectroscopy

Two background subtracted EPIC pn light curves of IGR J19140+0951 in two energy ranges are shown in Fig. 3, together with their hardness ratio. A clear hardening is present during the last half of the exposure, where the source intensity is increasing. Given the hardness ratio variability along the EPIC exposure, we extracted 4 time-selected spectra (for each camera) from 4 time intervals, as shown in Fig. 3. A joint fit of pn, MOS1 and MOS2 spectra with an absorbed power-law model (see Fig. 5) or adopting a simple absorbed black body, resulted in the parameters reported in Table 1. In the same Table (last column) we also report the spectroscopy of the time-averaged spectrum extracted from the whole 40 ks exposure.

Besides the flux, there is evidence for a variability in the hardness (power-law photon index or black body temperature), while the absorbing column density remains constant within the uncertainties (see Figs. 6 and 7). Therefore, we next fixed the absorbing column density to the value obtained in the time-averaged spectroscopy, and re-fitted the joint pn, MOS1, MOS2 spectra with a power-law or a black body. The results obtained with a fixed column density are reported in the same table. The spectral hardening with increasing flux near the end of the observation is even more evident in this case.

4 DISCUSSION

We reported here on the results of a 40 ks *XMM-Newton* observation of the HMXB IGR J19140+0951, and on the re-analysis of *Chandra* archival data. The main result of our work is the discovery of QPOs in the mHz frequency regime in the *XMM-Newton* observation, together with a periodicity in *Chandra* data that could be ascribed to the spin period of the NS. Since there are several issues about IGR J19140+0951 that we would like to discuss, we organize the discussion in different sub-sections, for clarity.

4.1 Is IGR J19140+0951 associated with EXO 1912+097?

Several papers in literature (Hannikainen et al. 2004, Hannikainen et al. 2007, in't Zand et al. 2004, in't Zand et al. 2006) proposed an association of IGR J19140+0951 with a poorly known EXOSAT source, EXO 1912+097. We show the sky region in Fig. 8, and report in Table 2 the coordinates of X–ray sources detected by different missions. We note that there is a typo in the WFC source coordinates reported in the text by in't Zand et al. 2004 (while the sky position is correctly shown in the figures by in't Zand et al. 2004, 2006). Therefore, we list in Table 2 also the correct WFC source coordinates (in't Zand 2016, private communication), for clarity.

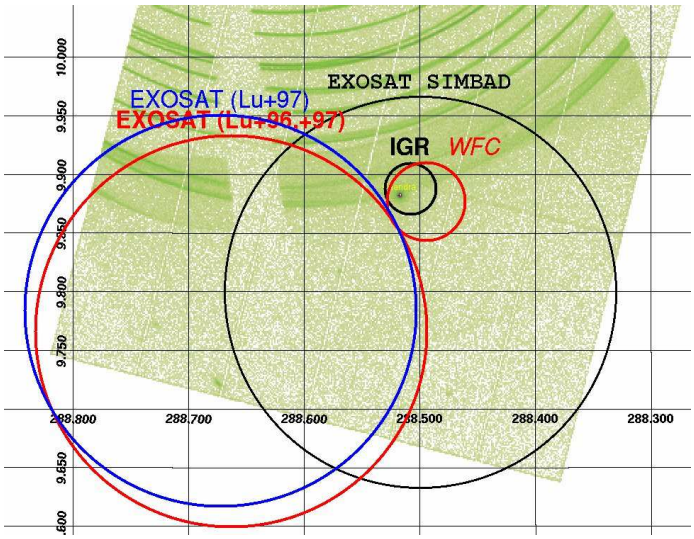

Figure 8. *XMM-Newton* EPIC pn image, together with the sky positions (and error circles as reported in Table 2) of sources detected by different missions. The *Chandra* position coincides with the *XMM-Newton* source. Equatorial coordinates are in units of degrees (J2000 equinox).

Since in literature there is some discrepancy in the EXOSAT source sky coordinates and its associated uncertainty is also unclear, we summarize here the two original papers that reported this detection: Lu et al. (1996) and Lu et al. (1997) (this latter available only in Chinese).

Lu et al. (1996) analysed EXOSAT Medium Energy array (ME; 2-6 keV) scans of the Galactic plane using a direct demodulation method. They listed only the source Galactic position, with no associated positional uncertainty (that we report in row n.4 of Table 2). An updated analysis of the same data, together with their statistical investigation, was reported in a later paper (Lu et al. 1997), where a *bootstrap* method was used to derive the source centroid and its uncertainty. This source position from the original EXOSAT data reported by the 1997 paper is listed in Table 2 (row n. 5). In row n. 6 we list the new centroid and its associated error radius derived from the *bootstrap* method (Lu et al. 1997). From a visual inspection of the EXO 1912+097 map (source 1 in Fig. 6 by Lu et al. 1997), we can derive an error radius of $\sim 10'$ (at 95% confidence level) in the source position.

Finally, SIMBAD reports different celestial coordinates for EXO 1912+097 (as already noted by in't Zand et al. 2004, 2006). This is puzzling, since the reference paper quoted by the SIMBAD website for the source sky coordinates is indeed Lu et al. (1996). We report them in Table 2 (and in Fig. 8) as well, but with the caveat that they are likely wrong or, at least, of unknown origin. Our feeling is that the SIMBAD source coordinates are simply rounded values from the EXOSAT name of the source.

To conclude, the *Chandra* position is only marginally consistent with the EXOSAT source reported by Lu and collaborators (1996, 1997), being outside the EXOSAT 95% error circle.

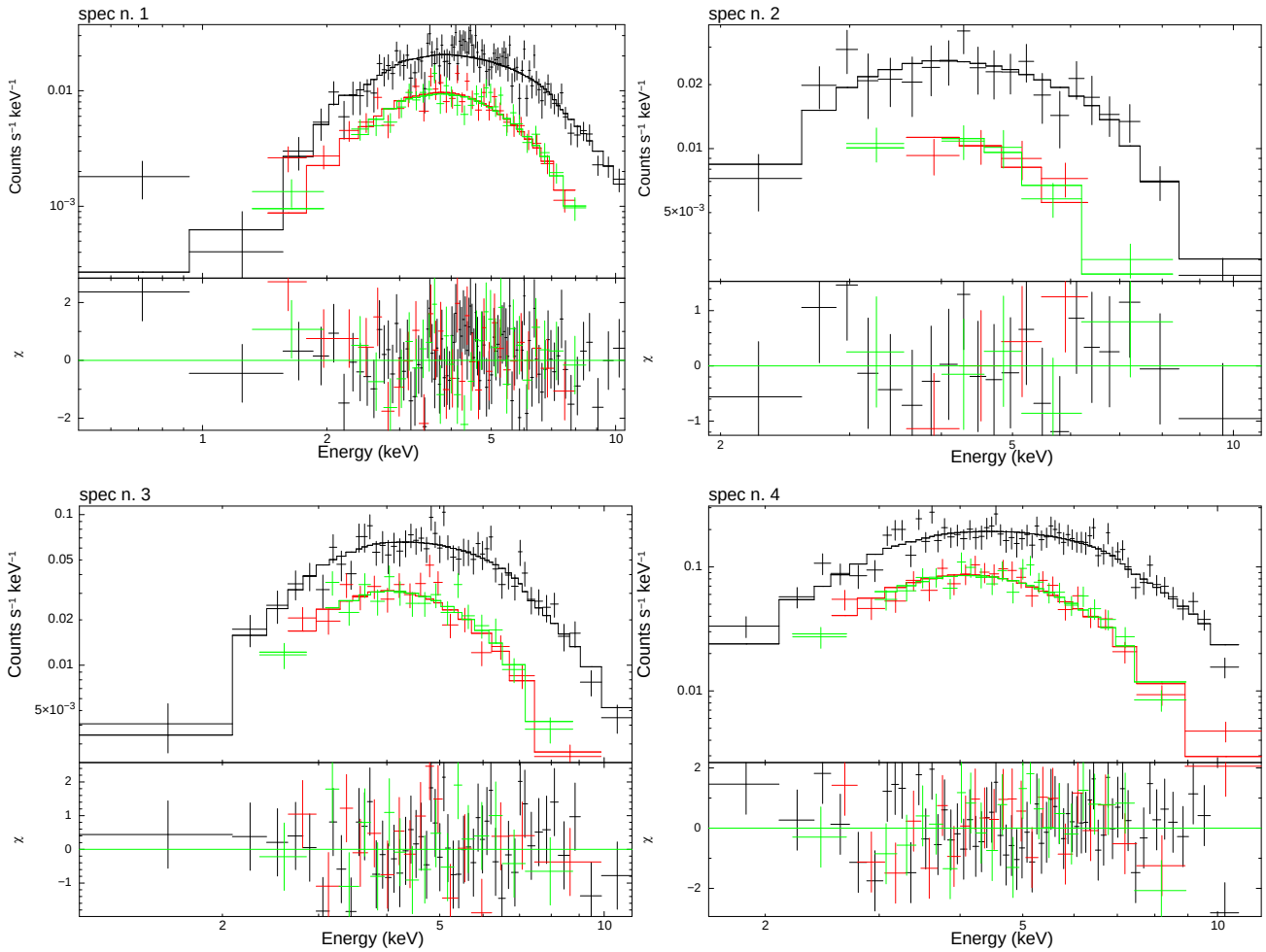

Figure 5. Spectral results from the temporal selected analysis. The four spectra correspond to the results reported in Table 1 for the power-law model. From left to right, top to bottom, count spectra number 1, 2, 3 and 4 are shown, together with their residuals in units of standard deviations from the power-law best-fit. In each panel, the upper spectrum (in black) marks EPIC pn, while lower spectra (in red and green) indicate MOS1 and MOS2, respectively.

4.2 Did *XMM-Newton* catch an X–ray eclipse?

XMM-Newton observed a very low level of X–ray emission from IGR J19140+0951 during the first ∼30 ks of the observation. This is the faintest state ever observed in this HMXB (2×10^{-12} erg cm^{-2} s^{-1}, 2-10 keV), translating into a luminosity L_X=3×10^{33} erg s^{-1} at a distance of 3.6 kpc (Torrejón et al. 2010). This could rise the question of a possible eclipse of the X–ray source by the supergiant companion. The rise in intensity approaching the end of the observation could suggest the eclipse egress. Assuming the ephemeris MJD 51593.4±0.32 (epoch of maximum flux assuming a sinusoidal model) with the period of 13.558 ±0.004 days ($RXTE$/ASM; Corbet et al. 2004) the *XMM-Newton* observation spanned an orbital phase interval $\Delta\phi$=0.51-0.54 (±0.12, extrapolating the uncertainties of 0.004 days on the orbital period to the present epoch). This implies that the *XMM-Newton* observation falls near the minimum of the orbital light curve (ϕ=0 is the maximum in the light curve). However, the orbital profile reported by Wen et al. (2006) ($RXTE$/ASM), does not show any evidence for an eclipse during the X–ray minimum. Moreover, the investigation of the variability of the intrinsic absorption along the orbit indicates a non-eclipsing system with a binary inclination around 65° (Prat et al. 2008). Also our *XMM-Newton* spectroscopy disfavours the possibility of an eclipse: the X–ray spectrum of the very faint initial part of the observation does not show any of the typical properties of the scattered X-ray emission observed during an eclipse: an emerging iron line with a large equivalent width and a lower absorption compared to out-of-eclipse X-ray emission (because the scattering into the line of sight is by less dense wind material (Haberl 1991)). A prolonged absorption dip lasting the first half of the observation is also excluded, since the absorbing column density does not show evidence for variability along the whole observation.

Therefore, we conclude that the low intensity is intrinsic to the source, leading to at least 1000 the source dynamic range with respect to previous observations: Rodriguez et al. (2005) report on an X–ray flux, corrected for the absorption, reaching 2×10^{-9} erg cm^{-2} s^{-1} in the 1-20 keV energy range (see also Rodriguez et al. 2006 for another dim state, although 10 times brighter than what we observed with *XMM-Newton*).

4.3 IGR J19140+0951: an intermediate case between SFXTs and persistent HMXBs?

It is worth noting that a high dynamic range of 3 orders of magnitude in an HMXB is more typical of a Supergiant Fast X-ray

Table 1. Results of the temporal selected (EPIC pn, MOS 1 and MOS 2) spectroscopy with two simple models, an absorbed power-law (PEGPWRLW in XSPEC) and an absorbed black body model. Numbers identify the temporal selected spectra as in Fig. 3, while the last column reports on the time-averaged spectroscopy. Flux is in the 2–10 keV energy range in units of 10^{-12} erg cm^{-2} s^{-1} and is corrected for the absorption, $L_{2-10keV}$ is the X-ray luminosity in units of 10^{33} erg s^{-1} (assuming a 3.6 kpc distance), N_H (in units of 10^{22} cm^{-2}; TBABS model in XSPEC with Wilms et al. (2000) abundances). Black body temperature, kT_{bb}, is in keV. Black body radius, R_{bb}, is in km at 3.6 kpc. The uncertainties on $L_{2-10keV}$ include only the 90% error on the unabsorbed flux.

Power-law param	1	2	3	4	Time-averaged
N_H	$11.6^{+1.3}_{-1.1}$	14^{+4}_{-3}	15^{+2}_{-2}	$12.6^{+1.7}_{-1.5}$	$12.8^{+0.8}_{-0.7}$
Γ	$1.72^{+0.18}_{-0.17}$	$1.8^{+0.4}_{-0.4}$	$1.6^{+0.2}_{-0.2}$	$1.20^{+0.17}_{-0.16}$	$1.56^{+0.09}_{-0.09}$
Unabs. Flux	1.98 ± 0.08	2.8 ± 0.3	7.6 ± 0.4	21.6 ± 0.9	3.89 ± 0.09
$L_{2-10keV}$	3.1 ± 0.1	4.3 ± 0.5	11.8 ± 0.6	33.5 ± 1.4	6.0 ± 0.1
χ^2_ν/dof	1.088/146	0.649/25	0.983/79	1.013/104	1.126/292
Power-law param	1	2	3	4	
N_H	12.8 fixed	12.8 fixed	12.8 fixed	12.8 fixed	
Γ	$1.86^{+0.09}_{-0.09}$	$1.66^{+0.21}_{-0.21}$	$1.37^{+0.10}_{-0.10}$	$1.22^{+0.09}_{-0.09}$	
Unabs. Flux	2.11 ± 0.05	2.64 ± 0.14	6.9 ± 0.2	21.7 ± 0.5	
χ^2_ν/dof	1.097/147	0.631/26	1.024/80	1.004/105	
BB param	1	2	3	4	Time-averaged
N_H	$6.1^{+0.7}_{-0.7}$	$6.6^{+2.6}_{-2.2}$	$8.2^{+1.3}_{-1.2}$	$7.0^{+1.0}_{-0.9}$	$6.8^{+0.5}_{-0.4}$
kT_{bb}	$1.67^{+0.09}_{-0.08}$	$1.82^{+0.26}_{-0.21}$	$1.90^{+0.14}_{-0.13}$	$2.17^{+0.14}_{-0.13}$	$1.89^{+0.06}_{-0.06}$
R_{bb}	$0.053^{+0.006}_{-0.005}$	$0.053^{+0.017}_{-0.010}$	$0.080^{+0.010}_{-0.010}$	$0.120^{+0.010}_{-0.010}$	$0.061^{+0.004}_{-0.003}$
χ^2_ν/dof	1.075/146	0.655/25	0.992/79	0.949/104	1.113/292
BB param	1	2	3	4	
N_H	6.8 fixed	6.8 fixed	6.8 fixed	6.8 fixed	
kT_{bb}	$1.62^{+0.06}_{-0.06}$	$1.81^{+0.18}_{-0.15}$	$2.0^{+0.1}_{-0.1}$	$2.2^{+0.1}_{-0.1}$	
R_{bb}	$0.057^{+0.004}_{-0.003}$	$0.054^{+0.009}_{-0.007}$	$0.073^{+0.006}_{-0.005}$	$0.120^{+0.007}_{-0.007}$	
χ^2_ν/dof	1.084/147	0.630/26	1.031/80	0.941/105	

Table 2. X–ray sources detected by different X–ray missions, with their coordinates and position uncertainties.

Observations	R.A. (J2000)	Dec. (J2000)	Error (& conf. level)	Ref.
Chandra	$19^h14^m4\overset{s}{.}232$	$+9°52'58\overset{''}{.}29$	$0\overset{''}{.}6$	in't Zand et al. 2006
INTEGRAL	$19^h14^m2\overset{s}{.}$	$+9°53.3'$	$1.3'$ (90%)	Cabanac et al. 2004
BeppoSAX/WFC	$19^h13^m58\overset{s}{.}8$	$+9°52'37''0$	$2'$ (90%)	in't Zand 2016 (priv. comm.)
EXOSAT/ME (EXO 1912+097; $l = 44\overset{\circ}{.}26$, $b = -0\overset{\circ}{.}65$)	$19^h14^m39\overset{s}{.}2$	$+9°45'59\overset{''}{.}4$	none	Lu et al. 1996
EXOSAT/ME (DD 1911+098; $l = 44\overset{\circ}{.}28$, $b = -0\overset{\circ}{.}65$)	$19^h14^m41\overset{s}{.}47$	$+9°47'03\overset{''}{.}2$	none	Lu et al. 1997
EXOSAT/ME (n.1 in Lu97 Table 5; $l = 44\overset{\circ}{.}26$, $b = -0\overset{\circ}{.}65$)	$19^h14^m39\overset{s}{.}2$	$+9°45'59\overset{''}{.}4$	$10'$ (95%)	Lu et al. 1997
EXO 1912+097	$19^h14^m00\overset{s}{.}$	$+9°48'00\overset{''}{.}0$	none	SIMBAD

Transient (SFXT; see Sidoli 2013 for a review) rather than of a persistent HMXB with a supergiant donor (SgHMXB). In SFXTs the dynamic range is larger than 100 and it is one of the characterizing properties of the class, together with the low duty cycle (a few %) of their transient and luminous (L>a few 10^{35} erg s^{-1}) X-ray emission (see, e.g., Paizis & Sidoli 2014). Rodriguez et al. (2005), from *RXTE* and *INTEGRAL* observations, already pointed out a substantial variability of the source intensity. We searched in the public *INTEGRAL* archive (12.3 yrs of data; Paizis et al. 2013) to get an estimate of the source duty cycle at hard X–rays: the source position falls within the *INTEGRAL*/IBIS FOV (within 12° from the centre) for about 9.68 Ms, and the source is detected for only 12% of the time in the hard band 17–50 keV. We can compare this duty cycle of 12% (17–50 keV), with what observed with *INTEGRAL* from other kinds of SgHMXBs (all at similar distances, 2-4 kpc), reported by Paizis & Sidoli (2014): the percentage of time spent in activity increases, starting from the most extreme SFXTs (∼0.1%), to the intermediate SFXTs (∼3-5%), to the transient SgHMXB 4U 1907+09 (∼23%), up to the persistent, eclipsing, SgHMXBs Vela X-1 and 4U 1700-377 (76-79%). These latter two sources are basically always detected by *INTEGRAL* when they are not in eclipse. Interestingly, the transient "not so transient" source 4U 1907+09 was suggested to be a sort of missing link between SFXTs and persistent SgHMXB because of its intermediate level of activity (Doroshenko et al. 2012). This behaviour was confirmed at hard X-rays with *INTEGRAL* (Paizis & Sidoli 2014). In this respect, IGR J19140+0951 might be another example of a

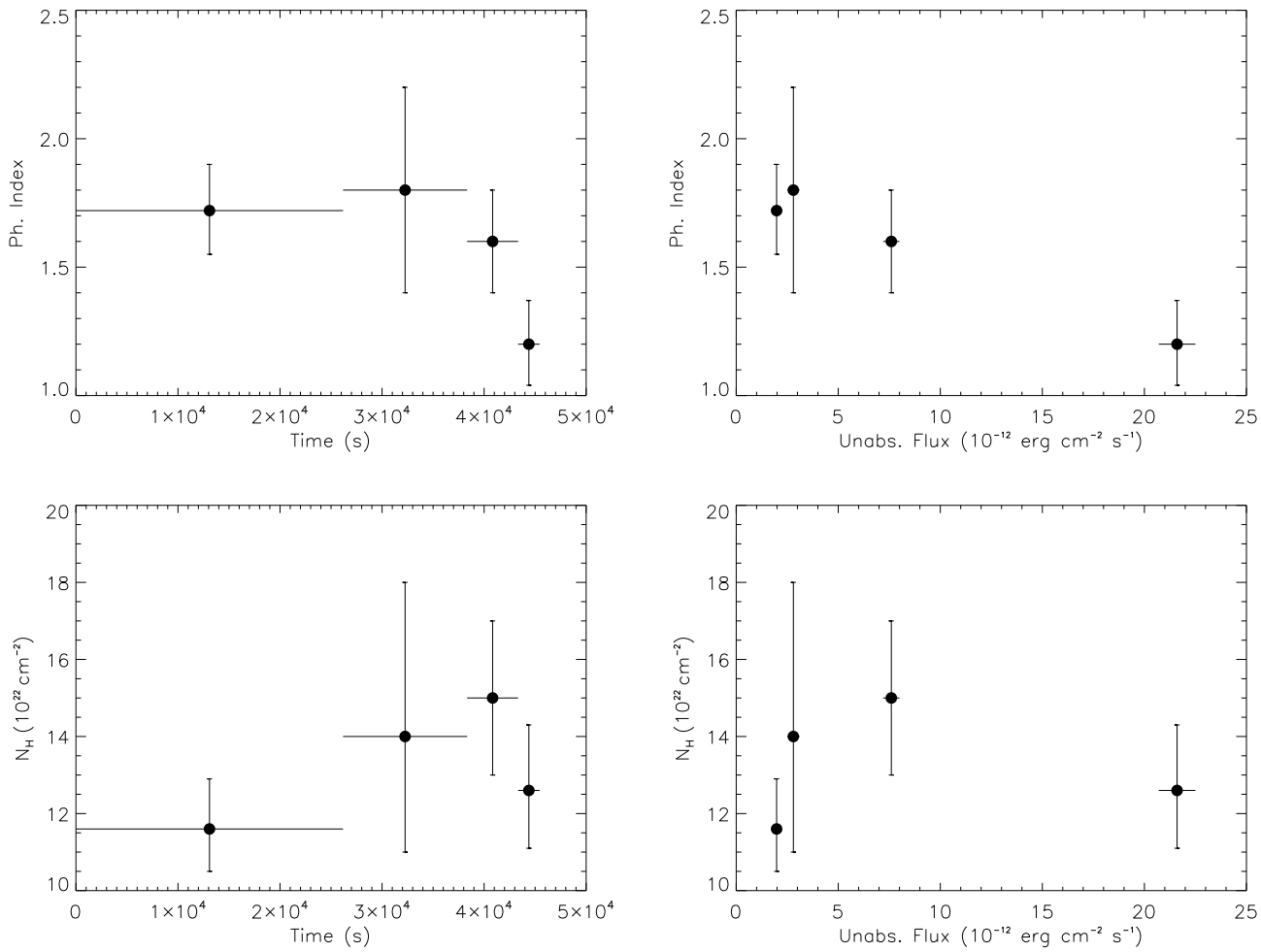

Figure 6. EPIC time-resolved spectroscopy using an absorbed power-law model (Table 1).

very variable SgHMXB, suggesting a smooth transition between SFXTs and persistent SgHMXBs.

4.4 Quasi-periodic oscillations

We discovered QPOs in IGR J19140+0951 during the *XMM-Newton* observation, with the strongest peak at a frequency of 1.46±0.07 mHz, together with its second and third harmonics (Fig. 4), in the second part of our observation, at an X-ray luminosity $\sim 10^{34}$ erg s^{-1}. Given its very low frequency, the total exposure of our observations limits prevented us from a further investigation of its evolution within the *XMM-Newton* observation. However, its absence in $Chandra$ data indicates a transient nature.

QPOs in the range 1 mHz-20 Hz have been observed in several HMXB pulsars, with persistent and transient X–ray emission (Finger 1998), both with Be and early type supergiant companions (see James et al. (2010) for a list of sources). Usually these features are transient. QPOs are also present in low mass X-ray binaries (LMXBs), but at much higher frequencies, in the kHz range (van der Klis 1998). The most popular models explaining QPOs (both in LMXB and HMXBs) assume the existence of an accretion disc. While the Roche-lobe-overflow (RLO) in LMXBs guarantees the formation of a disc, in HMXBs with no RLO its presence is much more elusive and debated: steady spin-up phases are usually taken as an evidence for it, while random walk spin behavior is believed to indicate a wind-fed system. Spin-up phases are often observed in Be/XRBs systems during their transient luminous outbursts, where an accretion disc is assumed to form from the dense slow wind coming from the Keplerian decretion disc of the massive Be companion. In HMXBs with supergiant companions with radially outflowing fast winds, the presence of a disc is posed into question. Usually, both the short term variability of the X–ray flux and the pulsar spin period evolution, point to accretion from the companion wind. However, we will discuss QPOs in both kinds of accretion.

Typically, the QPO feature is interpreted as a diagnostic of the inner radius of the accretion disc feeding the NS and of its interaction with the pulsar magnetosphere: it could be either the signature of the Keplerian frequency of an accreting inhomogeneity moving at the magnetospheric radius, r_m (ν_{QPO}=ν_k(r_m); Keplerian frequency model, hereafter KM; van der Klis 1999), or its beat frequency with the NS spin (ν_{QPO}=ν_k(r_m)-ν_{spin}; beat frequency model, BFM; Alpar & Shaham 1985, Lamb et al. 1985).

If the periodicity we detected in $Chandra$ data is really the pulsar spin period, in IGR J19140+0951 the frequency ν_{QPO} is

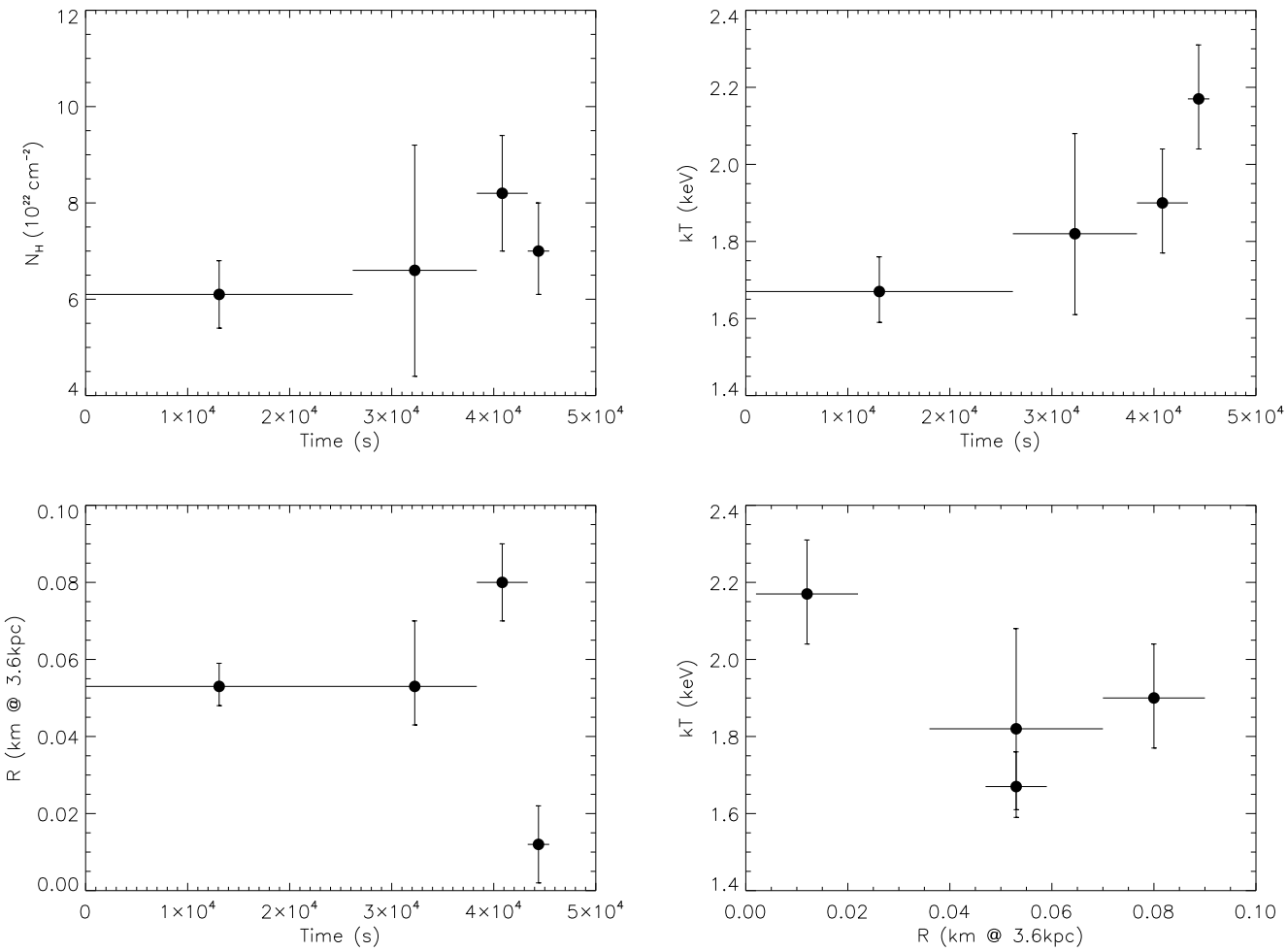

Figure 7. EPIC time-resolved spectroscopy using an absorbed black body model (Table 1).

much larger than ν_{spin}, so both BFM and KM predict a similar Keplerian frequency, ν_k, at the inner disc radius, r_{in}. Since

$$r_{in} = \left(\frac{GM}{4\pi^2\nu_k^2}\right)^{1/3} \quad (1)$$

assuming a NS mass, M, of $1.4M_\odot$, this implies r_{in}=1.2-1.3$\times10^{10}$ cm in IGR J19140+0951. In accreting X–ray pulsars it is possible to assume $r_{in}\equiv r_m$, where r_m mainly depends on the NS dipole magnetic moment (μ) and on the mass accretion rate $\dot{M}$ (Ghosh & Lamb 1979):

$$r_m \equiv \eta\left(\frac{\mu^4}{GM\dot{M}^2}\right)^{1/7} = (4.7\times10^9\ \mathrm{cm})\,\eta\,\mu_{30}^{4/7}M_{1.4}^{-1/7}\dot{M}_{13}^{-2/7}, \quad (2)$$

where $M = (1.4\ M_\odot)M_{1.4}$ is the NS mass, η∼0.5-1, $\dot{M} = (10^{13}\,\mathrm{g\,s^{-1}})\dot{M}_{13}$ is the accretion rate, and $\mu_{30} = \mu/(10^{30}\ \mathrm{G\,cm^3})$. Therefore, in the BFM (and KM) framework, the above value for r_m together with the measured time-averaged X-ray luminosity of $L_{2-10keV}$=6$\times10^{33}$ erg s^{-1} during the *XMM-Newton* observation (see Table 1), leads to a NS magnetic field strength B∼(1-4)$\times10^{13}$ G.

To allow accretion, r_m should be lower than the corotation radius (r_{cor}=$(GMP_{spin}^2/(4\pi^2))^{1/3}$), the radial distance where the plasma in the disc corotates with the NS. Under the already considered hypothesis that the spin period is really $P_{spin} = 5\,937\pm219$ s, we obtain a large corotation radius r_{cor}=5.4-5.6$\times10^{10}$ cm, which indeed enables accretion. Since there is no independent constraint on the pulsar magnetic field, we are not able to draw any unambiguous conclusion about the QPO interpretation.

However, given the supergiant donor (where a fast outflowing wind typically reaches a terminal velocity around 1000 km s^{-1}) and its wide orbit (∼13.5 days), a wind-fed system is a more plausible picture for IGR J19140+0951. In this case, a quasi-spherical settling accretion model for slow X–ray pulsars is applicable (Shakura et al. 2012). In slow X–ray pulsars with a low X–ray luminosity ($L_X<10^{35}$ erg s^{-1}) the wind matter captured within the Bondi radius of the NS remains hot and cannot efficiently penetrate the NS magnetosphere. It accumulates above the magnetospheric radius, forming a quasi static hot shell of matter. This extended quasi-static shell mediates both the accretion rate and the angular momentum transfer to (or removal from) the NS surface, by means of large-scale convective motions. The characteristic time-scale for these motions produces the appearence of QPOs just at the mHz frequencies (Shakura et al. 2012), in agreement with what we observed in *XMM-Newton* data.

The fact that the IGR J19140+0951 QPO has a second and a third (rather than a fourth) harmonic is quite curious (not easy to make odd harmonics), but this is not unheard of since it is also the case in many BH LMXBs. Indeed the nature of QPOs' higher harmonics is an open problem in BH binaries as well, where QPOs are very common features and are very well studied, especially at low frequencies.

It is worth noting that in all QPO models discussed above, the QPO frequency is expected to be correlated with the accretion rate. Assuming that the source flux is an appropriate proxy of the accretion rate, we expect to observe a higher QPO frequency at higher source fluxes. This seems to exclude an interpretation of the signal observed in the $Chandra$ data (0.17 mHz) as a QPO, because in this observation the flux was higher ($\sim 10^{-10}$ erg cm^{-2} s^{-1}) than during the *XMM-Newton* observation where the QPO frequency was 1.46 mHz. This favours the interpretation of the signal at $5\,937 \pm 219$ s as the NS spin period.

5 CONCLUSIONS

We discovered 1.46 mHz QPO (together with its second and third harmonics) from the HMXB IGR J19140+0951 with *XMM-Newton*, when the source was in a faint state ($\sim 10^{34}$ erg s^{-1}). Assuming the current models for the formation of QPOs in HMXBs (both in disc-fed and in wind-fed systems), given the long orbital period and the supergiant nature of the donor star (implying a fast outflowing wind), quasi-spherical accretion from the companion wind is favoured. In this latter scenario, the QPO is produced by the convective motions of material captured from the donor wind, that accumulates in a hot shell above the NS magnetosphere. Our reanalysis of a public $Chandra$ observation shows a modulation at $5\,937 \pm 219$ s, which we interpret as the spin period of the NS. The comparison between the low flux shown during the *XMM-Newton* observation and previous observations reported in literature, leads to about 3 orders of magnitude the dynamic range of the source intensity. It overlaps with the one observed from SFXTs, although the duty cycle of its luminous activity is not as extreme as in SFXTs. This suggests that IGR J19140+0951 is an intermediate system between them and the supergiant HMXBs with persistent X–ray emission.

ACKNOWLEDGMENTS

This work is based on data from observations with *XMM-Newton*. *XMM-Newton* is an ESA science mission with instruments and contributions directly funded by ESA Member States and the USA (NASA). The scientific results reported in this article are also based on data obtained from the *Chandra* Data Archive. This research has made use of software provided by the *Chandra* X-ray Center (CXC) in the application package CIAO, and of the SIMBAD database, operated at CDS, Strasbourg, France. This research has made use of the IGR Sources page maintained by J. Rodriguez (http://irfu.cea.fr/Sap/IGR-Sources/), and of the $INTEGRAL$ archive developed at INAF-IASF Milano, http://www.iasf-milano.inaf.it/∼ada/GOLIA.html. A. Paizis and K. Postnov are thanked for many interesting discussions. LS is grateful to J. in't Zand for help with the WFC source coordinates and for providing the text of the Chinese paper Lu et al (1997). LS thanks Silvia Sidoli for the translation of the Chinese paper Lu et al (1997) and acknowledges the grant from PRIN-INAF 2014, "Towards a unified picture of accretion in High Mass X-Ray Binaries" (PI: L. Sidoli). PE acknowledges funding in the framework of the NWO Vidi award A.2320.0076 (PI: N. Rea). SEM acknowledges the Glasstone research fellowship program.

REFERENCES

Alpar M. A., Shaham J., 1985, Nature, 316, 239
Balucinska-Church M., McCammon D., 1992, ApJ, 400, 699
Belloni T., Hasinger G., 1990, A&A, 230, 103
Belloni T., Psaltis D., van der Klis M., 2002, ApJ, 572, 392
Cabanac C., Rodriguez J., Hannikainen D., Lund N., Petrucci P.-O., Henri G., Durouchoux P., Schultz J., 2004, The Astronomer's Telegram, 272
Chaty S., Rahoui F., Foellmi C., Tomsick J. A., Rodriguez J., Walter R., 2008, A&A, 484, 783
Corbet R. H. D., Hannikainen D. C., Remillard R., 2004, The Astronomer's Telegram, 269
den Herder J. W., Brinkman A. C., Kahn S. M., Branduardi-Raymont G., Thomsen K., Aarts H., Audard M., Bixler J. V. e. a., 2001, A&A, 365, L7
Doroshenko V., Santangelo A., Ducci L., Klochkov D., 2012, A&A, 548, A19
Esposito P., Israel G. L., Milisavljevic D., Mapelli M., Zampieri L., Sidoli L., Fabbiano G., Rodríguez Castillo G. A., 2015, MNRAS, 452, 1112
Esposito P., Israel G. L., Sidoli L., Mapelli M., Zampieri L., Motta S. E., 2013, MNRAS, 436, 3380
Finger M. H., 1998, Advances in Space Research, 22, 1007
Ghosh P., Lamb F. K., 1979, ApJ, 234, 296
Haberl F., 1991, A&A, 252, 272
Hannikainen D. C., Rawlings M. G., Muhli P., Vilhu O., Schultz J., Rodriguez J., 2007, MNRAS, 380, 665
Hannikainen D. C., Rodriguez J., Cabanac C., Schultz J., Lund N., Vilhu O., Petrucci P. O., Henri G., 2004, A&A, 423, L17
Hannikainen D. C., Rodriguez J., Pottschmidt K., 2003, IAU Circ., 8088
in't Zand J., Heise J., Ubertini P., Bazzano A., Markwardt C., 2004, in Schoenfelder V., Lichti G., Winkler C., eds, 5th INTEGRAL Workshop on the INTEGRAL Universe Vol. 552 of ESA Special Publication, A BeppoSAX-WFC Viewpoint of New INTEGRAL Sources, Particularly IGR J17544-2619. p. 427
in't Zand J. J. M., Jonker P. G., Nelemans G., Steeghs D., O'Brien K., 2006, A&A, 448, 1101
Israel G. L., Stella L., 1996, ApJ, 468, 369
James M., Paul B., Devasia J., Indulekha K., 2010, MNRAS, 407, 285
Kuulkers E., 2005, in Burderi L., Antonelli L. A., D'Antona F., di Salvo T., Israel G. L., Piersanti L., Tornambè A., Straniero O., eds, Interacting Binaries: Accretion, Evolution, and Outcomes Vol. 797 of American Institute of Physics Conference Series, An absorbed view of a new class of INTEGRAL sources. pp 402–409
Lamb F. K., Shibazaki N., Alpar M. A., Shaham J., 1985, Nature, 317, 681
Leahy D. A., Darbro W., Elsner R. F., Weisskopf M. C., Kahn S., Sutherland P. G., Grindlay J. E., 1983, ApJ, 266, 160
Lu F., Li T., Wu M., Sun X., 1997, Acta Astronomica Sinica, 38, 56

Lu F. J., Li T. P., Sun X. J., Wu M., Page C. G., 1996, A&AS, 115, 395
Nespoli E., Fabregat J., Mennickent R., 2007, The Astronomer's Telegram, 983
Nespoli E., Fabregat J., Mennickent R. E., 2008, A&A, 486, 911
Paizis A., Mereghetti S., Götz D., Fiorini M., Gaber M., Regni Ponzeveroni R., Sidoli L., Vercellone S., 2013, Astronomy and Computing, 1, 33
Paizis A., Sidoli L., 2014, MNRAS, 439, 3439
Prat L., Rodriguez J., Hannikainen D. C., Shaw S. E., 2008, MNRAS, 389, 301
Rahoui F., Chaty S., Lagage P.-O., Pantin E., 2008, A&A, 484, 801
Rodriguez J., Beckmann V., Hannikainen D. C., Lebrun F., Shaw S. E., Willis D., 2006, The Astronomer's Telegram, 800
Rodriguez J., Cabanac C., Hannikainen D. C., Beckmann V., Shaw S. E., Schultz J., 2005, A&A, 432, 235
Shakura N., Postnov K., Kochetkova A., Hjalmarsdotter L., 2012, MNRAS, 420, 216
Sidoli L., 2013, ArXiv e-prints, 1301.7574
Strüder L., Briel U., Dennerl K., Hartmann R., Kendziorra E., Meidinger N., Pfeffermann E., Reppin C., et al. 2001, A&A, 365, L18
Swank J. H., Markwardt C. B., 2003, The Astronomer's Telegram, 128
Torrejón J. M., Negueruela I., Smith D. M., Harrison T. E., 2010, A&A, 510, A61
Turner M. J. L., Abbey A., Arnaud M., Balasini M., Barbera M., Belsole E., Bennie P. J., Bernard J. P., et al. 2001, A&A, 365, L27
van der Klis M., 1998, Advances in Space Research, 22, 925
van der Klis M., 1999, Astrophysical Letters and Communications, 38, 69
Wen L., Levine A. M., Corbet R. H. D., Bradt H. V., 2006, ApJS, 163, 372
Wilms J., Allen A., McCray R., 2000, ApJ, 542, 914

This paper has been typeset from a TEX/ LATEX file prepared by the author.